International Conference on Applied Energy 2019
Aug12-15, 2019, Västerås, Sweden
Paper ID: 0999

THERMODYNAMIC ANALYSIS OF SOLAR ORGANIC RANKINE CYCLE WITH TWO-STAGE EVAPORATION

Xiaoqiang Hong[1,2], Jingyu Cao[2,3], Zhanying Zheng[1], Jin Xuan[4], Michael K.H. Leung[1*]

[1] School of Architecture and Civil Engineering, Xiamen University, Xiamen 361005, China

[2] Ability R&D Energy Research Centre, School of Energy and Environment, City University of Hong Kong, Hong Kong, China

[3] Department of Thermal Science and Energy Engineering, University of Science and Technology of China, Hefei 230027, China

[4] Department of Chemical Engineering, Loughborough University, Loughborough, Leicestershire, U.K.

ABSTRACT

This paper presents thermodynamic analyses of a two-stage organic Rankine cycle (ORC) for solar thermal power generation. The effects of the operational parameters (i.e. high-pressure stage evaporating temperature, low-pressure stage evaporating temperature, solar collector outlet temperature and solar irradiation) on the SORC system performance (net power generation, overall system thermal efficiency, exergy efficiency and total thermal conductance) were investigated. The results indicated that there exist optimal high-pressure stage evaporating temperature and solar collector outlet temperature for maximizing the power generation, energy efficiency and exergy efficiency of the SORC system. As the solar irradiation and low-pressure stage evaporating temperature increase, the net power generation, overall system thermal efficiency and exergy efficiency increase.

Keywords: *Solar power; ORC; Thermodynamics; Two-stage evaporation.*

*Corresponding author. Tel.: +852-3442-4626; fax: +852-3442-0688
E-mail address: mkh.leung@cityu.edu.hk

1. INTRODUCTION

Solar thermal power systems have great potential for large scale applications [1]. One of the most feasible ways to produce electricity from solar thermal energy is to adopt Organic Rankine Cycle (ORC). In an ORC system, an organic fluid with low critical point is used instead of water as the working fluid. Such feature makes the solar-driven ORC (SORC) a suitable low-temperature thermal power system.

The ORC irreversibility involved in heat transfer process can be further reduced by using multiple-pressure evaporation [2,3]. In dual-pressure evaporation ORC, the evaporation process is split into two different pressure levels [4].

However, there is so far no report found in solar-driven two-pressure stage evaporation ORC. In this study, two-pressure stage evaporation ORC is integrated with solar heating to form a SORC system. The energy and exergy performances of the SORC were quantitatively analysed.

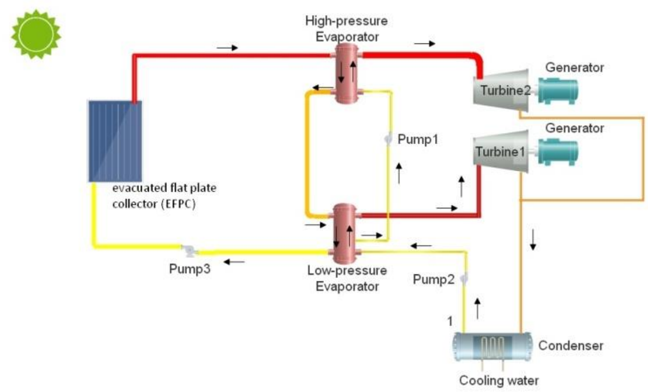

Fig. 1. Schematic diagram of solar ORC system.

2. SYSTEM DESCRIPTION

The schematic of the proposed system is illustrated in Figure 1. It is comprised of two elements, namely, the solar collectors and series two-stage organic Rankine cycle (STORC) sub-system. Non-concentrating collectors are used. Pressurized water is used as the heat transfer medium in solar system [5]. The STORC sub-system

Selection and peer-review under responsibility of the scientific committee of the 11th Int. Conf. on Applied Energy (ICAE2019).

comprises two evaporators, two expanders, two pumps and a condenser.

3. MATHEMATICAL ANALYSES

3.1 Solar collector modelling

The efficiency of solar collector, η_c, is calculated by [6]:

$$\eta_c = \eta_0 K_\theta - \frac{a}{G}(\mathrm{T}-\mathrm{T}_a) - \frac{b}{G}(\mathrm{T}-\mathrm{T}_a)^2 \quad (1)$$

where η_0 = 0.82; K_θ = 0.91; a = 0.399; and b = 0.0067 [7]. The exergy input of the system is define as [8]:

$$E_{in} = E_{solar} = A_c G[1+\frac{1}{3}\left(\frac{T_0}{T_{sun}}\right)^4 - \frac{4}{3}\left(\frac{T_0}{T_{sun}}\right)] \quad (2)$$

where T_{sun} is the sun temperature and equals to 6000K [9].

3.2 Dual-pressure stage evaporation Organic Rankine Cycle

The heat balances in evaporator 1 (low T) can be expressed as:

$$Q_{e1} = m_{wf,total}(\mathrm{h}_{5'}-\mathrm{h}_4)+\mathrm{m}_{wf,1}(\mathrm{h}_{1'}-\mathrm{h}_{5'}) \quad (3)$$

$$Q_{e1} = Q_{e1,pre} + Q_{e1,\mathrm{eva}} + Q_{e1,\mathrm{sup}} \quad (4)$$

The thermal conductance UA of the evaporator 1 is calculated by:

$$(\mathrm{UA})_{e1} = (\mathrm{UA})_{e1,pre} + (\mathrm{UA})_{e1,\mathrm{eva}} + (\mathrm{UA})_{e1,\mathrm{sup}} \quad (5)$$

$$(UA)_{e1,pre} = Q_{e1,pre} / \Delta T_{e1,pre} \quad (6)$$

$$(UA)_{e1,eva} = Q_{e1,\mathrm{eva}} / \Delta T_{e1,\mathrm{eva}} \quad (7)$$

$$(UA)_{e1,\mathrm{sup}} = Q_{e1,\mathrm{sup}} / \Delta T_{e1,\mathrm{sup}} \quad (8)$$

where ΔT is the log mean temperature difference calculated from the inlet and outlet temperatures of both fluids. The thermodynamic model of evaporator 2 (high T) is similar to evaporator 1. The heat flow at the condenser and cooling water is described by:

$$Q_c = m_{wf,\mathrm{total}}(\mathrm{h}_2-\mathrm{h}_3)=\mathrm{m}_{cw} c_{cw}(\mathrm{T}_{cw,out}-\mathrm{T}_{cw,\mathrm{in}}) \quad (9)$$

The thermal conductance in the condenser is given by:

$$(\mathrm{UA})_c = (\mathrm{UA})_{\mathrm{c},pre} + (\mathrm{UA})_{\mathrm{c,eva}} + (\mathrm{UA})_{\mathrm{c,sub}} \quad (10)$$

$$(UA)_{\mathrm{c},pre} = Q_{\mathrm{c},pre} / \Delta T_{\mathrm{c},pre} \quad (11)$$

$$(UA)_{\mathrm{c,con}} = Q_{c,\mathrm{cond}} / \Delta T_{\mathrm{c,con}} \quad (12)$$

$$(UA)_{\mathrm{c,sub}} = Q_{c,\mathrm{sub}} / \Delta T_{\mathrm{c,sub}} \quad (13)$$

The isentropic efficiencies of two expanders are assumed to be the same and defined as:

$$\eta_{\exp} = (h_{1'}-h_2)/(h_{1'}-h_{2s}) = (h_{1"}-h_2)/(h_{1"}-h_{2s}) \quad (14)$$

where h_{2s} is specific enthalpy at the turbine outlet experiencing an isentropic process. The total electricity generated by two expanders is calculated by using:

$$W_{\exp} = (m_{wf,1}(h_{1'}-h_2) + m_{wf,2}(h_{1"}-h_2))\eta_{ge} \quad (15)$$

where η_{ge} is efficiency of generator.

The isentropic efficiencies of two pumps in ORC are assumed to be the same and defined as:

$$\eta_{pump} = (h_{4s}-h_3)/(h_4-h_3) = (h_{7s}-h_{5'})/(h_7-h_{5'}) \quad (16)$$

The total power consumed by two feed pumps is:

$$W_{pump} = m_{wf,\mathrm{total}}(h_4-h_3) + m_{wf,2}(h_7-h_{5'}) \quad (17)$$

Thermal efficiency of the SORC:

$$\eta_{th} = W_{net}/(GA_c) \quad (18)$$

Exergy efficiency of the SORC:

$$\eta_{ex} = W_{net}/E_{in} \quad (19)$$

4. MODEL VALIDATION

In this study, the numerical simulation was performance in combination of Matlab and Refprop. To validate the model, the numerical solutions for STORC were compared with the literature results [10] which have been validated by experimental data. The results are listed in Table 1. It can be seen that the model can predict accurate thermal performance.

Table 1: Model validation for STORC

$T_{w,in}$ (°C)	T_{e2} (°C)	T_{e1} (°C)	$T_{w,mid}$	$T_{w,mid}$ of [9]	$T_{w,mid}$ Deviation
90	77	70	81.5	82	0.61%
95	80	71	84.2	84	0.21%
100	84	73	87.9	88	0.16%
105	87	74	90.4	90	0.42%
110	91	76	93.9	94	0.09%
115	95	78	97.4	97	0.41%
120	97	80	98.8	99	0.18%

5. RESULTS AND DISCUSSION

5.1 Impact of high-pressure stage evaporating temperature

In this analysis, the evaporating temperature of the high-pressure stage evaporator was varied from 85°C to 105°C while other parameters remain unchanged, i.e. low-pressure stage evaporating temperature at 75°C, collector outlet temperature of 120°C and solar irradiation of 800W/m^2. Simulation was carried out using the established mathematical model. The results are shown in Fig. 3. It is found that the net power generation, system thermal efficiency and exergy efficiency initially increase and decrease afterwards as the high-pressure stage evaporating temperature increases from 85°C to 105°C. Meanwhile, it can be seen that the total thermal conductance rises from 14600 to 18500 W/°C as the high-pressure stage evaporating temperature increases from 85 to 90°C.

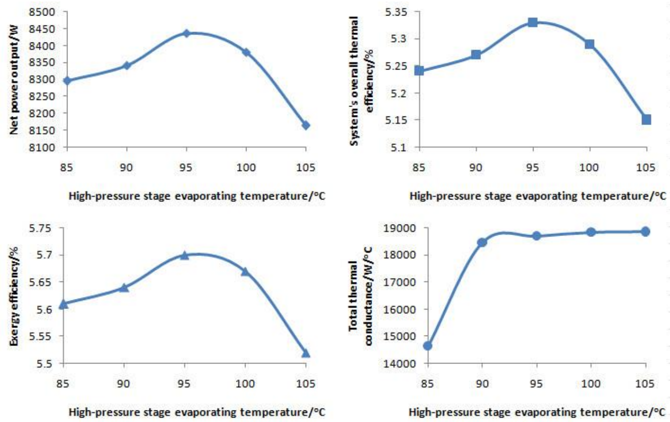

Fig. 3. Variation of net power output, thermal efficiency, exergy efficiency and total thermal conductance versus the high-pressure stage evaporating temperature.

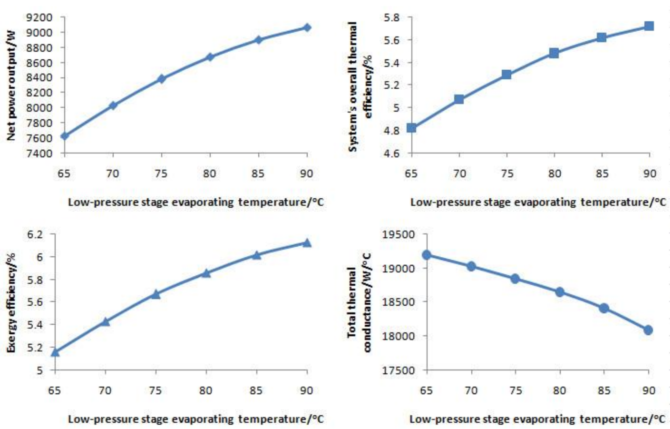

Fig. 4. Variation of net power output, thermal efficiency, exergy efficiency and total thermal conductance versus the low-pressure stage evaporating temperature.

5.2 Impact of low-pressure stage evaporating temperature

The effects of the evaporating temperature of the low-pressure stage evaporator are shown in Fig.4. It is found that increasing the low-pressure stage evaporating temperature leads to increases in net power generation, overall system thermal efficiency and exergy efficiency, but decrease in total thermal conductance. This is because that increasing low-pressure stage evaporating temperature helps increase the pressure difference between the low-pressure stage evaporator and condenser, resulting in enhanced thermal efficiency of the power generation.

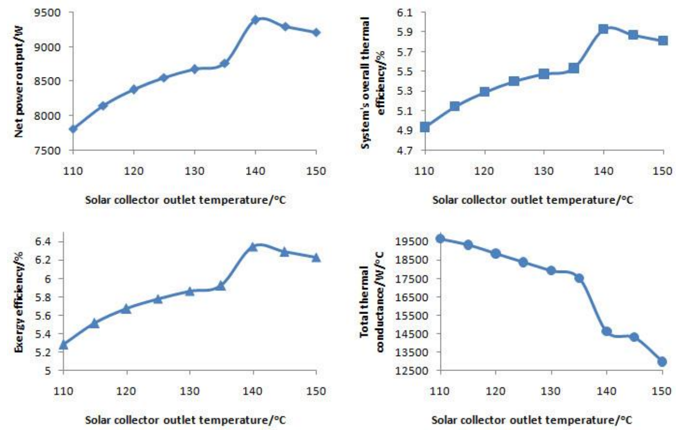

Fig. 5. Variation of net power output, thermal efficiency, exergy efficiency and total thermal conductance versus the solar collector outlet temperature.

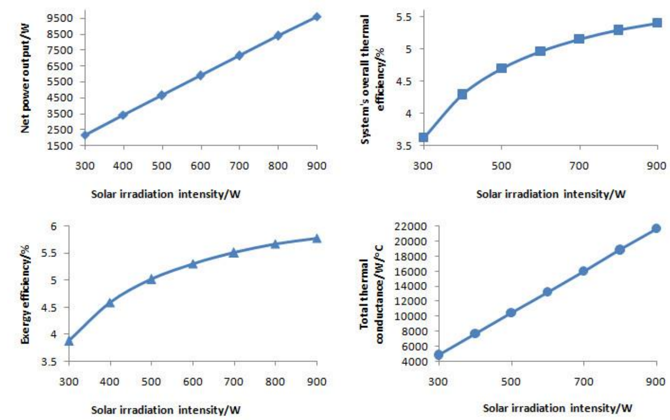

Fig. 6. Variation of net power output, thermal efficiency, exergy efficiency and total thermal conductance versus the solar irradiation.

5.3 Impact of solar collector outlet temperature

The effects of the collector outlet temperature are presented in Fig. 5. It can be seen that the net power generation, overall system thermal efficiency and exergy efficiency rise with the solar collector outlet temperature 140°C. The overall thermal conductance decreases with the collector outlet temperature above 140°C.

5.4 Impact of solar irradiation

Figure 6 shows the effects of the solar irradiation from 300 to 900W/m^2. It is found that increase in solar irradiation yields significant increases in net power generation, overall system thermal efficiency, exergy efficiency and overall thermal conductance. This is because higher solar irradiation implies more solar heat gain, which helped improve both ORC power generation and the system thermal efficiency.

6. CONCLUSION

Solar organic Rankine cycle with two-pressure stage evaporation has been evaluated by energy and exergy analyses. Based on the test results obtained under various system characteristic parameters and operational conditions, we found that: (1) the net power generation, thermal efficiency and exergy efficiency of the SORC system rise with the high-pressure stage evaporating temperature increasing from 85^{o}C to 95^{o}C and then drop after the temperature reaches 95^{o}C; (2) increases in low-pressure stage evaporating temperature and solar irradiation intensity lead to increases in net power generation, overall system energy efficiency and exergy efficiency; (3) the net power generation, thermal efficiency and exergy efficiency of the system rise with the solar collector outlet temperature and then drop after the temperature reaches 140^{o}C; (4) the total thermal conductance increases with high-pressure stage evaporating temperature and solar irradiation intensity, while decreases with low-pressure stage evaporating temperature and solar collector outlet temperature.

ACKNOWLEDGMENTS

This work was supported by the Natural Science Foundation of Fujian Province of China (2018J05086) and the Education Department of Fujian Province (B16151).

REFERENCES

[1] Aboelwafa O, Fateen S-EK, Soliman A, Ismail IM. A review on solar Rankine cycles: Working fluids, applications, and cycle modifications. Renewable and Sustainable Energy Reviews. 2018;82:868-85.

[2] Lecompte S, Huisseune H, van den Broek M, Vanslambrouck B, De Paepe M. Review of organic Rankine cycle (ORC) architectures for waste heat recovery. Renewable and Sustainable Energy Reviews. 2015;47:448-61.

[3] Li J, Ge Z, Duan Y, Yang Z, Liu Q. Parametric optimization and thermodynamic performance comparison of single-pressure and dual-pressure evaporation organic Rankine cycles. Applied energy. 2018;217:409-21.

[4] Stijepovic MZ, Papadopoulos AI, Linke P, Grujic AS, Seferlis P. An exergy composite curves approach for the design of optimum multi-pressure organic Rankine cycle processes. Energy. 2014;69:285-98.

[5] Kutlu C, Li J, Su Y, Pei G, Riffat S. Off-design performance modelling of a solar organic Rankine cycle integrated with pressurized hot water storage unit for community level application. Energy Conversion and Management. 2018;166:132-45.

[6] Freeman J, Hellgardt K, Markides CN. Working fluid selection and electrical performance optimisation of a domestic solar-ORC combined heat and power system for year-round operation in the UK. Applied energy. 2017;186:291-303.

[7] Calise F, d'Accadia MD, Vicidomini M, Scarpellino M. Design and simulation of a prototype of a small-scale solar CHP system based on evacuated flat-plate solar collectors and Organic Rankine Cycle. Energy Conversion and Management. 2015;90:347-63.

[8] Wang M, Wang J, Zhao P, Dai Y. Multi-objective optimization of a combined cooling, heating and power system driven by solar energy. Energy Conversion and Management. 2015;89:289-97.

[9] Al-Sulaiman FA, Dincer I, Hamdullahpur F. Exergy modeling of a new solar driven trigeneration system. Solar Energy. 2011;85:2228-43.

[10] Li T, Zhang Z, Lu J, Yang J, Hu Y. Two-stage evaporation strategy to improve system performance for organic Rankine cycle. Applied energy. 2015;150:323-34.